

Identification of proteases that regulate erythrocyte rupture by the malaria parasite *Plasmodium falciparum*

Shirin Arastu-Kapur¹, Elizabeth L Ponder², Urša Pečar Fonovič¹, Sharon Yeoh³, Fang Yuan^{1,6}, Marko Fonovič^{1,4}, Munira Grainger³, Carolyn I Phillips², James C Powers⁵ & Matthew Bogyo¹

Newly replicated *Plasmodium falciparum* parasites escape from host erythrocytes through a tightly regulated process that is mediated by multiple classes of proteolytic enzymes. However, the identification of specific proteases has been challenging. We describe here a forward chemical genetic screen using a highly focused library of more than 1,200 covalent serine and cysteine protease inhibitors to identify compounds that block host cell rupture by *P. falciparum*. Using hits from the library screen, we identified the subtilisin-family serine protease PfSUB1 and the cysteine protease dipeptidyl peptidase 3 (DPAP3) as primary regulators of this process. Inhibition of both DPAP3 and PfSUB1 caused a block in proteolytic processing of the serine repeat antigen (SERA) protein SERA5 that correlated with the observed block in rupture. Furthermore, DPAP3 inhibition reduced the levels of mature PfSUB1. These results suggest that two mechanistically distinct proteases function to regulate processing of downstream substrates required for efficient release of parasites from host red blood cells.

Malaria is a devastating disease that causes significant mortality in many countries of the developing world. The most deadly form of the disease is caused by the pathogen *P. falciparum*. Significant efforts have been made to understand the process by which the parasite invades a host cell to establish infection, yet relatively little is known about the process by which the parasite mediates its release after replication has occurred. This process is essential for propagation of the pathogen, and agents that block rupture are likely to be valuable for development as new antimalarial drugs.

Proteolytic enzymes are key regulators of a number of important biological processes in virtually all organisms. They also are viable drug targets; there are many protease-directed small-molecule therapeutics currently in use for the treatment of human diseases ranging from hypertension to cancer. The use of both selective and broad-spectrum inhibitors as well as genetic studies have helped to identify several proteases as regulators of the process of invasion^{1,2}. For the process of host cell rupture, broad-spectrum inhibitors clearly point to a critical role for both serine and cysteine proteases, yet direct identification of proteases that regulate this process has not been possible^{3,4}.

A number of proteins are proteolytically processed during the process of host cell invasion and rupture. Multiple cell surface receptors are shed during invasion, and several of these proteins are processed just before or during parasite release from the host cell^{1,5–8}. The SERAs make up a family of nine proteins that have been extensively studied as possible vaccine candidates. Several members

of this family (SERA4, SERA5 and SERA6) are abundantly expressed in the parasitophorous vacuole of the late-stage blood form of the parasite and are proteolytically processed and released into the extracellular environment upon rupture^{9–12}. Furthermore, deletion of any of the predominant blood stage proteins (SERA4, SERA5 and SERA6) is lethal¹⁰, and deletion of the insect stage-expressed family member SERA8 leads to a complete block of sporozoite release from oocytes⁹. Combined with studies showing that antibodies against SERA5 block parasite egress¹³, these results suggest that the SERAs are potentially important regulators of host cell rupture.

In this study we describe the use of a unique library of covalent, irreversible serine and cysteine protease inhibitors to identify compounds that induce a specific block in release of the parasite from host red blood cells. Using a class of chloroisocoumarins and peptide vinyl sulfone hits from the screen, we identified the serine protease PfSUB1 and the cysteine protease DPAP3 as key regulators of host cell rupture. Inhibition of either of these protease targets caused an accumulation of the unprocessed intermediates of SERA5, and this block in processing directly correlated with a block in parasite release from the host. Notably, specific inhibition of DPAP3 prevented the formation of mature PfSUB1 and also blocked the production of an unrelated secretory protein (AMA-1). Based on these data, we propose that PfSUB1 and DPAP3 both regulate parasite release from host erythrocytes by ultimately facilitating the processing of the downstream mediator SERA5.

¹Department of Pathology and ²Department of Microbiology and Immunology, Stanford University School of Medicine, 300 Pasteur Drive, Stanford, California 94305, USA. ³Division of Parasitology, National Institute for Medical Research, The Ridgeway, Mill Hill, London NW7 1AA, UK. ⁴Department of Biochemistry, Molecular and Structural Biology, Jozef Stefan Institute, Jamova 39, SI-1000 Ljubljana, Slovenia. ⁵Department of Chemistry, Georgia Institute of Technology, 901 Atlantic Drive, Atlanta, Georgia 30332, USA. ⁶Present address: EnzMed (Nanjing) Co., Ltd., 28 Hengjing Road, Nanjing, China 210046. Correspondence should be addressed to M.B. (mbogyo@stanford.edu).

Received 14 November 2007; accepted 8 January 2008; published online 3 February 2008; doi:10.1038/nchembio.70

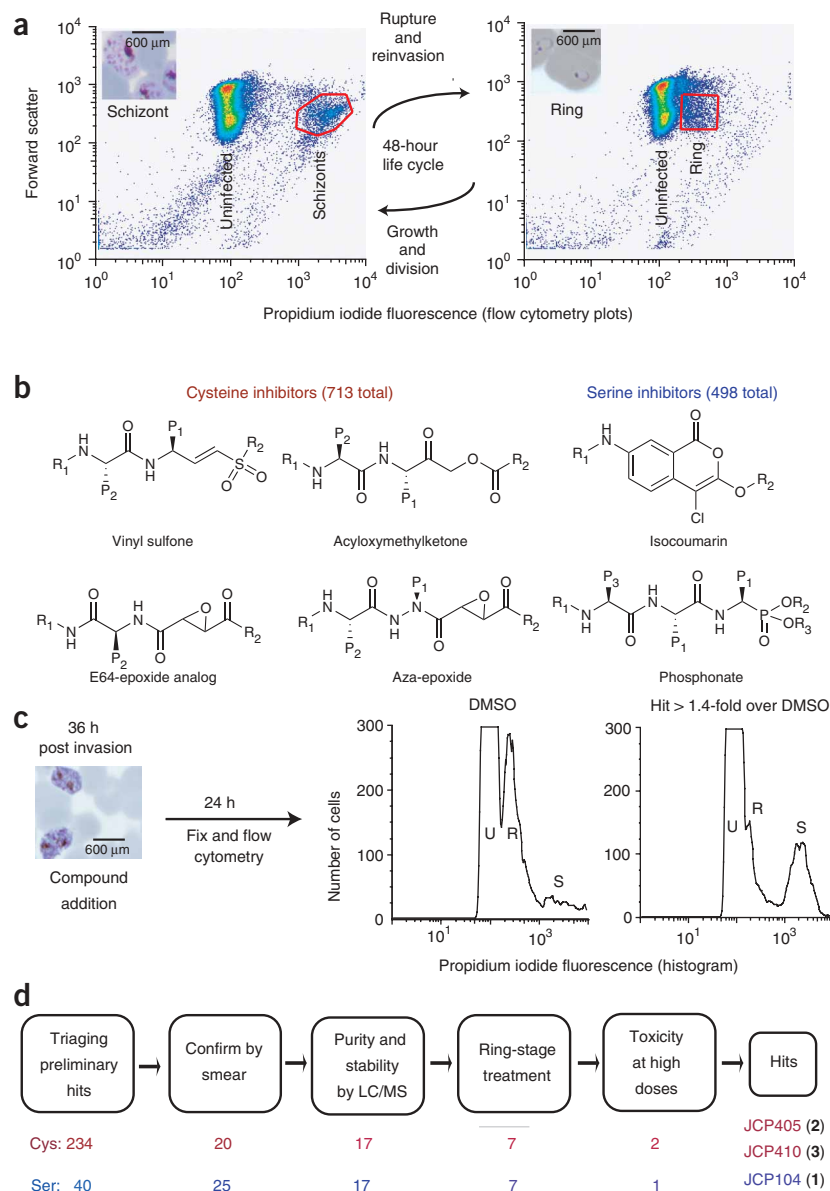


Figure 1 Assembly and screening of the protease inhibitor library. **(a)** Dot plots of synchronous ring- and schizont-stage cultures of *P. falciparum* stained with propidium iodide and plotted as propidium iodide fluorescence relative to forward scatter of white light. The distinct life cycle stages are shown boxed in red. Giemsa-stained thin blood smear images of the respective life cycle stages are shown in the inset. **(b)** General structures of the main classes of covalent cysteine and serine protease inhibitors in the library used for screening. The library contained 498 serine and 713 cysteine protease-directed compounds. P₁ and P₂ are side chains of P1 and P2 amino acids. **(c)** Synchronous cultures of *P. falciparum* at early schizont stage were treated with compounds at a final concentration of 10 μ M. Cells were fixed for analysis by flow cytometry 24 h later. Compounds that exhibited a > 1.4-fold accumulation of cells detected in the schizont gate relative to DMSO controls in at least two of three runs were selected as initial hits. Histograms for a representative DMSO control and hit compound are shown. U, uninfected; R, ring stage; S, schizont stage. **(d)** Preliminary hits were confirmed by blood smear to eliminate compounds that were not reproducible or that exhibited an abnormal morphology. The remaining compounds were analyzed for purity and aqueous stability. Stable and pure compounds were used to treat ring-stage parasites to eliminate hits that exhibited general effects on parasite development. Compounds that caused hemolysis or gross toxicity at higher concentrations (50 μ M) were eliminated. The total numbers at each stage of triage are shown. The final hits were JCP104, JCP405 and JCP410.

content) allows specific populations of infected RBCs to be counted (Fig. 1a).

We initially assembled a library of 1,211 irreversible small-molecule protease inhibitors from collections synthesized in the Bogoy and Powers laboratories, as well as compounds from W. Roush (The Scripps Research Institute). The complete set of compound

structures and plate locations were uploaded into a web-based database system established by Collaborative Drug Discovery (www.collaborativedrug.com). This system allows compound structures to be linked to plate locations and assay data using a web browser interface. It also provides a simple way to share screening data with collaborators. The final library was made up of the cysteine protease-specific peptide vinyl sulfones, acyloxymethyl ketones, aza-epoxides and epoxysuccinates, and the serine protease-specific chloroiso-coumarins and peptide phosphonates (Fig. 1b). We specifically chose scaffolds that inhibited target proteases by formation of a permanent covalent bond¹⁶ so that they could be easily used for target identification. The complete set of compounds was screened by addition of each compound to synchronized cultures of D10 parasites at 36 h post invasion (schizont stage). Cultures were treated with vehicle alone (DMSO) or compounds (10 μ M final) for 24 h, and then cultures were fixed and stained for analysis by FACS (Fig. 1c). After performing the screen in triplicate, compounds that caused a greater than 1.4-fold accumulation of schizont-stage parasites relative to the

RESULTS

Assembly and screening of the small-molecule library

After establishing an initial infection in the liver, *P. falciparum* establishes a blood-stage life cycle in which it exclusively invades red blood cells (RBCs). The blood stages can be grown *in vitro*, and parasites can be synchronized using a number of commonly used methods¹⁴. Once in synchronous growth, parasites cycle together through the multiple blood stages (merozoite, ring, trophozoite and schizont) over a 48 h time period. Their progress through each of these morphological stages can be monitored microscopically using simple staining methods. However, in order to be able to quantitatively monitor large populations of parasites, we turned to a previously described fluorescence-activated cell scanning (FACS) method in which parasite populations can be quantitatively monitored¹⁵. Because infected RBCs lack a nucleus and the parasite replicates its DNA multiple times in the late schizont stage, simple measurement of forward scatter (to monitor general cell morphology and size) relative to propidium iodide staining (to measure DNA

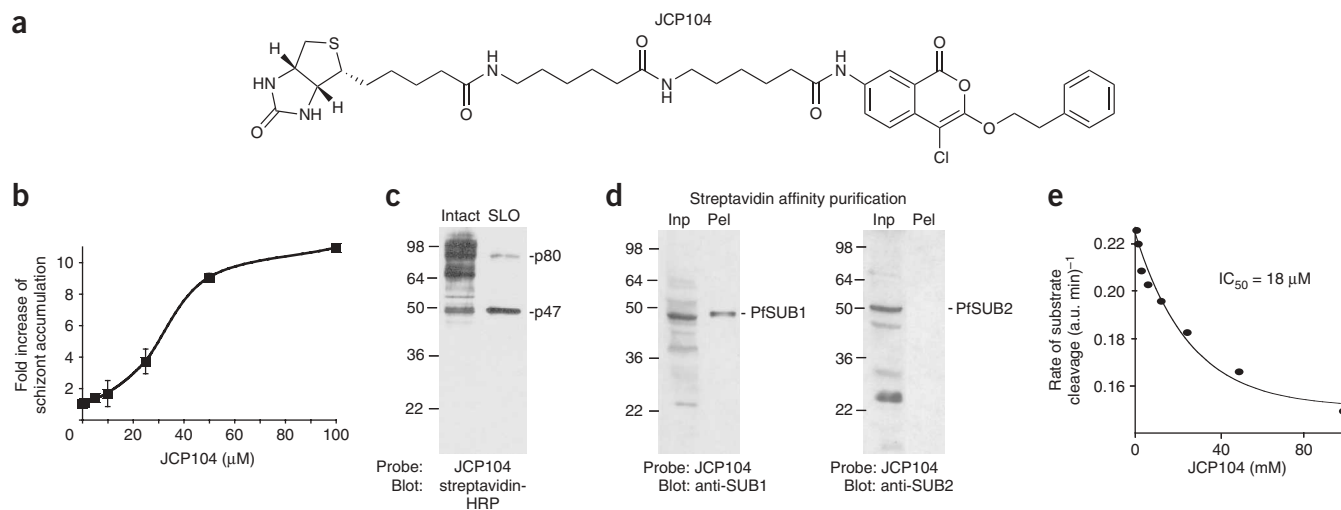


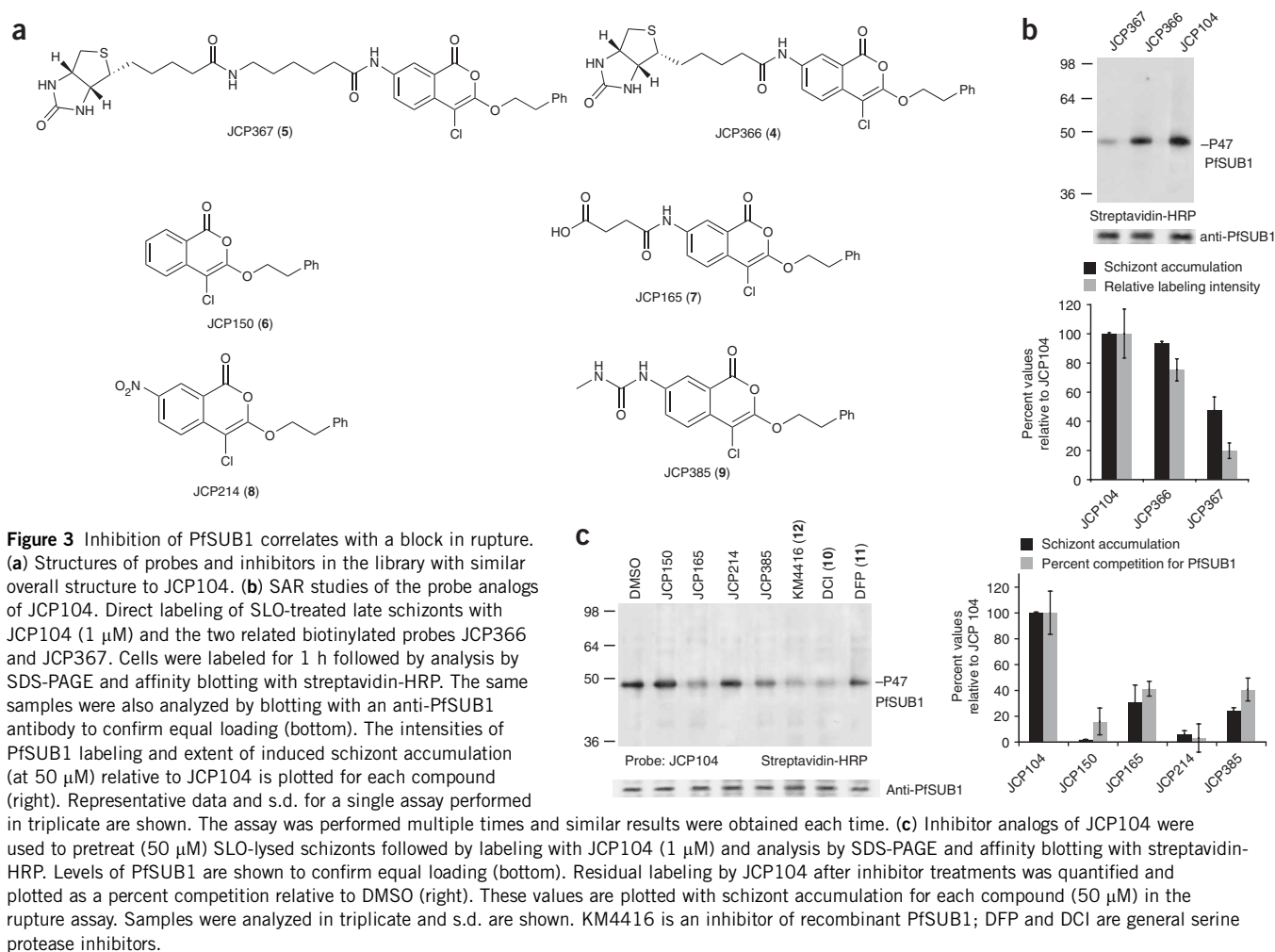
Figure 2 Identification of PfSUB1 as the target of JCP104. **(a)** Structure of JCP104, the biotinylated chloroisocoumarin identified as the optimal serine protease hit in the flow cytometry-based rupture assay. **(b)** Dose response of JCP104 in the rupture assay. Synchronous parasite cultures at 36 h post invasion were treated in triplicate with dilutions of 1–100 μM JCP104, and the accumulation of schizonts was quantified by flow cytometry. Average fold increase of schizont accumulation relative to the DMSO control is plotted for each drug concentration. Samples were analyzed in triplicate with standard error bars shown. **(c)** Labeling of intact parasites with JCP104. Intact and SLO-treated schizonts that were labeled with 1 μM JCP104 were subsequently separated by 12% SDS-PAGE and analyzed by biotin affinity blotting using streptavidin-HRP. The predominant 47 kDa labeled protein observed in both SLO-treated and intact schizonts is indicated. **(d)** Identification of PfSUB1 as the target of JCP104. Schizont lysates solubilized in 1% nonidet P-40 were labeled with JCP104 (1 μM), and biotinylated proteins were collected on streptavidin agarose beads. Input samples (inp) before addition of streptavidin beads and pellet fractions (pel) eluted from the beads were analyzed by SDS-PAGE followed by blotting with mouse anti-PfSUB1 (left) and rabbit anti-PfSUB2 (right) anti-sera. **(e)** Dose-dependent inhibition of recombinant PfSUB1 cleavage of the fluorescent substrate pepF1-6R by JCP104. An IC_{50} value was calculated based on the curve fit shown.

DMSO control population in at least two of the replicates were counted as preliminary hits. These hits were then further triaged through a series of secondary assays in which compound purity, stability and effects at high concentrations and at different stages of the blood-stage life cycle were measured (Fig. 1d). Parasite morphology was closely monitored by smear analysis, which allowed assessment of overall phenotypic effects of the compounds on both the parasite and host red blood cells (Supplementary Fig. 1 online). Though we identified a number of compounds that appeared to induce a rupture defect by FACS analysis, some of these compounds seemed to be toxic to the parasites at high concentrations as judged by an overall condensed cell morphology. We also tested the final hits to confirm that they did not induce general toxicity to host cells using a simple cytotoxicity assay in BSC-1 cells (Supplementary Fig. 2 online). As a final test we examined the effects of the compounds on parasite growth when added to ring-stage parasites. All of the secondary triaging steps provided qualitative data that could be used to select the top hits for further analysis. In the end, we selected the chloroisocoumarin JCP104 (1) as the top serine protease inhibitor and the two peptide vinyl sulfones JCP405 (2) and JCP410 (3) (Fig. 1d) as our lead cysteine protease inhibitors for follow-up studies to identify target proteases. All three of these compounds induced a clear defect in parasite rupture that led to a reduction in the subsequent levels of ring-stage parasites (Supplementary Fig. 3 online) without inducing changes in schizont morphology or affecting ring-to-schizont development.

Identification of PfSUB1 as the target of JCP104

The chloroisocoumarin JCP104 (Fig. 2a) was retested over a range of concentrations to further confirm the rupture phenotype (Fig. 2b). These data indicated that JCP104 induces a block in rupture with an effector concentration for half-maximum response (EC_{50}) value of

22 $\mu\text{M} \pm 7 \mu\text{M}$. Because JCP104 already contained a biotin tag, we could use it to directly identify the target protease. Intact schizonts were treated with JCP104 for 1 h, and total protein extracts were analyzed by SDS-PAGE followed by affinity blotting for biotin using streptavidin-horse radish peroxidase (HRP). In parallel, schizont samples were treated with streptolysin O (SLO) to permeabilize the RBC plasma membrane without disrupting the parasitophorous vacuolar membrane (PVM)¹⁷ before JCP104 treatment. This allowed removal of highly abundant red cell proteins before treatment with JCP104. SLO treatment also caused enhanced delivery of JCP104 to the parasitophorous vacuole because the PVM allows diffusion-mediated passage of molecules smaller than M_w 1,200 (ref. 18). In addition, SLO treatments have been previously used to deliver non-cell-permeant biotinylated compounds to the parasitophorous vacuole¹⁹. The labeling pattern observed for both the intact and SLO-treated schizont-infected RBCs showed strong labeling of a 47 kDa protein (Fig. 2c). Upon SLO treatment only the 47 kDa protein and a second 80 kDa species were clearly labeled by JCP104. A search through the literature identified the subtilisin-family serine protease PfSUB1 as a possible target. This protease is proteolytically processed from an 80 kDa precursor through a P56 intermediate form to a mature 47 kDa form that is released upon rupture^{20–22}. Furthermore, attempts to knock out this protease in *P. falciparum* blood stages have been unsuccessful, which suggests that it has an essential role in the blood-stage life cycle of the parasite²³. To determine whether the labeled species included PfSUB1, we used antibodies specific to PfSUB1 as well as antibodies to a related subtilisin-like protease (PfSUB2) that has a role in shedding of surface proteins during invasion^{5,6}. After labeling of saponin-treated schizont-stage infected RBCs with JCP104, probe-labeled proteins were collected by affinity purification using streptavidin resin, and input and pellet



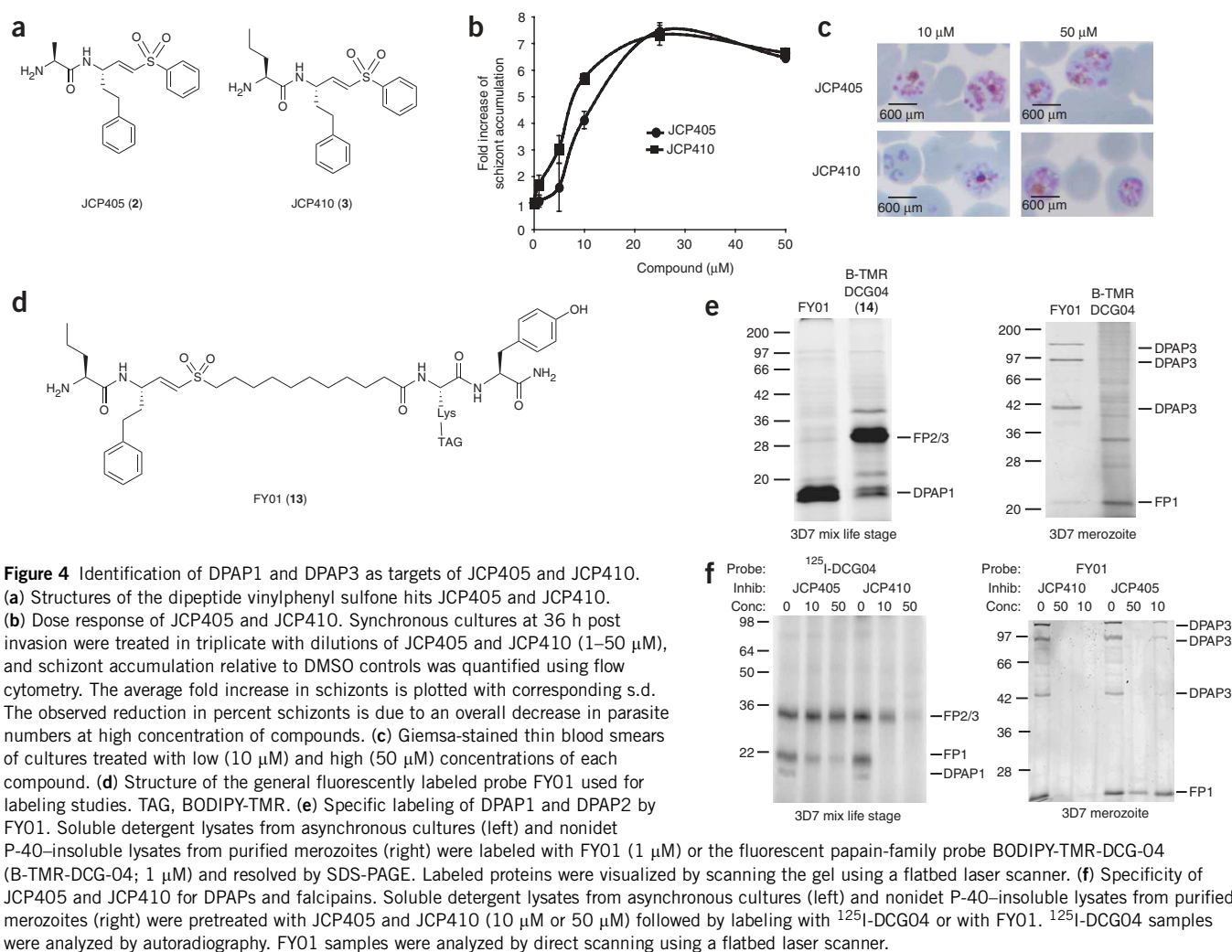
samples were probed with the PfSUB1 and PfSUB2 antibodies (Fig. 2d). These results suggest that the predominantly labeled 47 kDa target of JCP104 is the mature form of PfSUB1. Subsequently, we were also able to identify the 47 kDa protein by affinity purification with JCP104 followed by in-gel digestion and mass spectrometry-based sequencing (Supplementary Fig. 4 online). Finally, we tested the ability of JCP104 and several related negative control chloroisocoumarins to block the activity of recombinant PfSUB1 in a fluorogenic peptide substrate cleavage assay. Only JCP104, and not the inactive analogs, effectively inhibited the recombinant enzyme. The half-maximal inhibitory concentration (IC_{50}) value for JCP104 inhibition of PfSUB1 was determined to be 18 μ M (Fig. 2b), which is in line with the EC_{50} of this compound in the rupture assay (22 μ M; Fig. 2e).

JCP104 blocks rupture by inhibition of PfSUB1

We searched the library of serine protease inhibitors to find compounds that could be used to define a structure activity relationship (SAR) of JCP104 analogs for PfSUB1 binding (Fig. 3a). Two of the analogs (JCP366 (4) and JCP367 (5)) were nearly identical to JCP104, except that they contained either one or no amino hexanoic acid spacers between the isocoumarin and the biotin tag. Labeling of SLO-treated schizont-infected RBCs with JCP104 and these two compounds showed that JCP367 weakly labeled PfSUB1, whereas JCP366 was an effective label of PfSUB1 (Fig. 3b). When the

compounds were retested in the rupture assay and total schizont accumulation was quantified at a higher dose (50 μ M) than was used in the initial screen (10 μ M), both of the analogs induced a rupture defect. Importantly, the relative potency of these compounds in the rupture assay exactly correlated with the relative intensity of labeling of PfSUB1 in intact schizonts (Fig. 3b).

We next analyzed additional JCP104 analogs that could be tested for potency against PfSUB1 in intact schizonts using a simple competition assay (Fig. 3c). We tested four JCP104 analogs (JCP150 (6), JCP165 (7), JCP214 (8) and JCP385 (9)) as well as two well-characterized serine protease inhibitors: dichloroisocoumarin (DCI, 10) and diisopropylfluorophosphonate (DFP, 11). DCI is a relatively potent inhibitor of PfSUB1, whereas DFP shows virtually no activity²². We also included the small-molecule inhibitor KM4416 (12), which was identified in a screen of diverse small molecules for inhibitors of PfSUB1 (M. Blackman, UK National Institute for Medical Research, personal communication). All the positive control inhibitors induced a substantial reduction in labeling of PfSUB1 by JCP104, whereas the negative control DFP showed little or no effect (Fig. 3c). The chloroisocoumarin analogs showed different levels of competition for PfSUB1 labeling. Again, the overall relative potency of the compounds in the rupture assay exactly correlated with their ability to target PfSUB1 in the competition labeling assay. We also analyzed the dose response of all six compounds over a concentration range from 1 to



50 μ M to confirm that these SAR patterns were consistent across a range of inhibitor concentrations (Supplementary Fig. 5 online).

JCP405 and JCP410 target DPAP1 and DPAP3

The screen of the cysteine protease inhibitors produced a considerable number of hits, however many of these compounds induced a food vacuole defect as a result of their inhibition of the cysteine proteases falcipain-2 and falcipain-3 (refs. 3,24–27). Close analysis of the structures of the cysteine protease inhibitor hits that produced a specific rupture defect without any food vacuole effects drew our attention to two dipeptide vinyl sulfones, JCP405 and JCP410 (Fig. 4a). These compounds induced a potent, dose-dependent block in parasite rupture without altering parasite morphology (Fig. 4b,c). Both of these compounds were initially synthesized as inhibitors of the dipeptidyl peptidase cathepsin C (ref. 28). The *P. falciparum* genome contains three dipeptidyl peptidases (DPAP1, PF11_0174; DPAP2, PFL2290w; DPAP3, PFD0230c) with homology to human cathepsin C. Though very little is known about the functions of DPAP2 and DPAP3, biochemical and genetic studies suggest that DPAP1 has an important role in late-stage degradation of hemoglobin in the food vacuole²⁹. Our group has recently developed a highly selective probe, FY01 (13), that targets human cathepsin C (ref. 30). This probe is nearly identical in structure to both JCP405

and JCP410 (Fig. 4d). We therefore used this probe to monitor binding of compounds to the endogenous DPAP proteases of *P. falciparum*. We initially tested labeling of mixed-stage parasite extracts with FY01 and compared this labeling to the general broad-spectrum papain-family probe B-TMR-DCG-04 (14), which has previously been shown to target falcipain-1, falcipain-2 and falcipain-3 as well as DPAP1 (ref. 31; Fig. 4e). FY01 specifically labeled a 20 kDa doublet that was previously identified as DPAP1 in DCG04 labeling experiments³¹. We further confirmed the specific labeling of DPAP1 in mixed parasite extracts by immunoprecipitation using DPAP1-specific antibodies (Supplementary Fig. 6a online). When FY01 was used to label detergent-insoluble extracts from merozoite-stage parasites, three proteins at 120, 95 and 42 kDa were clearly labeled (Fig. 4e). These proteins were isolated by affinity purification using a biotin-labeled version of FY01. Mass spectrometry-based sequencing of each of these proteins identified all three as forms of DPAP3 (Supplementary Fig. 6b–d). We did not observe labeling of DPAP2, which is consistent with its proposed expression only in the sexual stages²⁹. Because the FY01 probe efficiently labeled DPAP3, we could use this probe to monitor potency of our hit compounds for this target, and we could use the general probe DCG04 to monitor the selectivity of the hits for DPAP1 relative to falcipain-1, falcipain-2 and falcipain-3 (Fig. 4f). Both JCP405 and JCP410 were effective

inhibitors of DPAP3 and DPAP1, but both also showed some level of cross-reactivity for falcipain-1, falcipain-2 and falcipain-3 (Fig. 4f). This cross-reactivity is not surprising as the falcipains are related papain-fold cysteine proteases that bind aliphatic P2 residues such as norleucine and alanine found on JCP405 and JCP410 (ref. 31).

JCP405 and JCP410 block rupture by inhibition of DPAP3

Because both JCP405 and JCP410 effectively inhibited both DPAP1 and DPAP3, we needed to develop compounds that could distinguish between these two proteases. Using the previously reported solid-phase synthesis method³², we generated a small library of dipeptide vinyl sulfones based on the FY01 structure in which the P2 amino acid was scanned through a set of natural and non-natural amino acids

(Fig. 5a). This library of 40 compounds was screened for potency against DPAP1 and DPAP3, and for falcipain-1, falcipain-2 and falcipain-3, using a competition assay with the general probes DCG04 and FY01 (Fig. 5a). The compound d12 (15), which contains the non-natural amino acid nitrotyrosine in the P2 position, was selected for follow-up studies because it showed the greatest specificity for DPAP3 relative to DPAP1. In addition, we selected the compound containing a P2 proline residue (16) as the most optimal DPAP1-selective inhibitor. These two P2 residues were then used to make the DPAP3-selective inhibitor SAK1 (17) and the DPAP1-selective inhibitor SAK2 (18; Fig. 5b).

Competition studies in purified intact schizonts using the FY01 probe allowed us to assess the specificity of SAK1 and SAK2 for

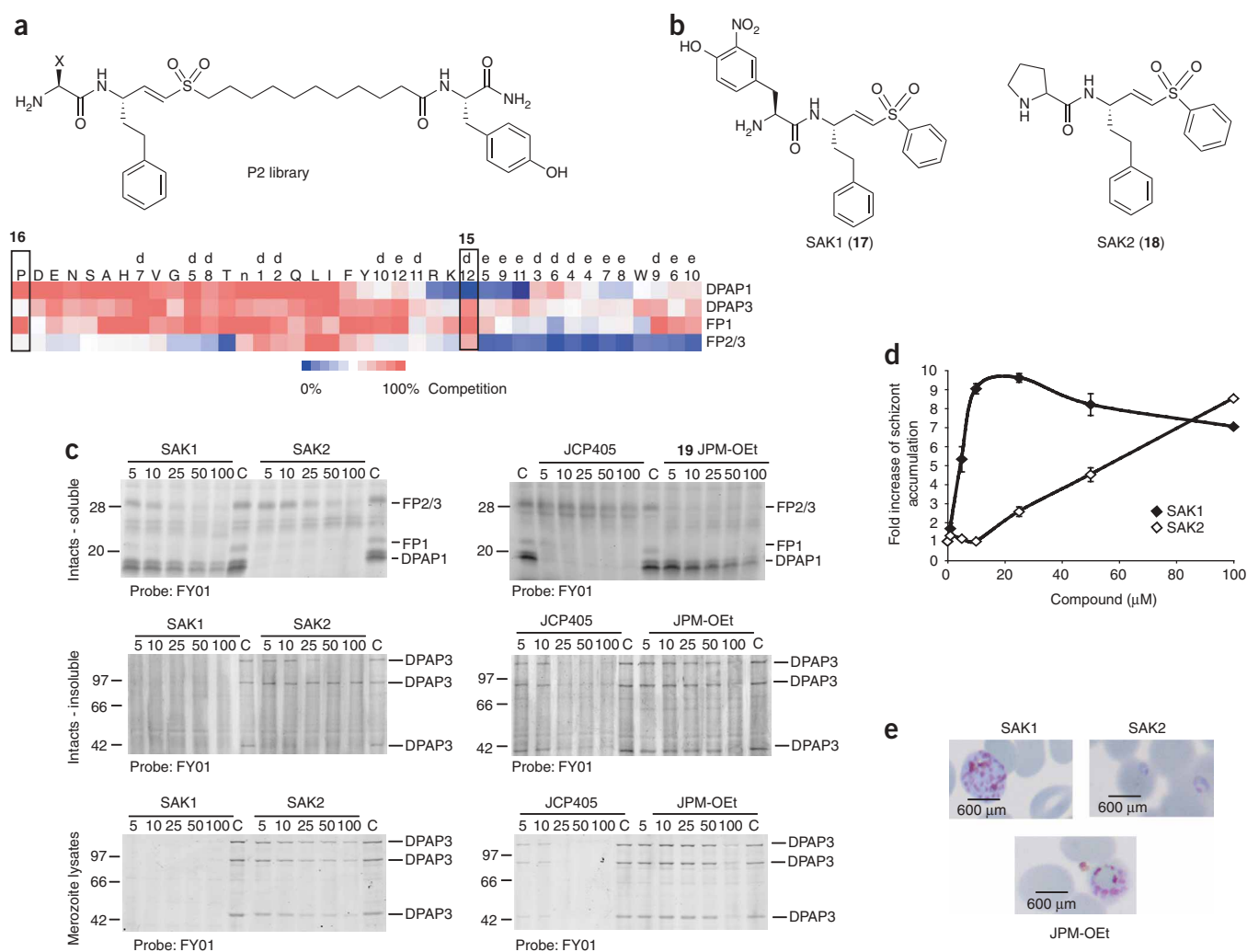


Figure 5 Design of selective DPAP3 and DPAP1 inhibitors. **(a)** The vinyl sulfone library used to identify selective inhibitors is made up of 40 inhibitors that contain natural (indicated by standard one-letter codes) and non-natural (noted with 'd' or 'e' and a number) amino acids at the variable X position. The library was screened (100 μ M) in mixed lysates (to detect DPAP1 and falcipain-1, falcipain-2 and falcipain-3) and in nonidet P-40-insoluble merozoite lysates (to detect DPAP3) using a competition labeling assay with ¹²⁵I-DCG-04 or FY01, respectively. A heat map of residual protease activity is shown. The d12 and proline P2 compounds are highlighted because they exhibited desired selectivity patterns. **(b)** Structures of the vinyl sulfones SAK1 (DPAP3 selective) and SAK2 (DPAP1 selective) synthesized based on data in **a**. **(c)** Intact schizonts were treated with a range of concentrations (5–100 μ M) of SAK1, SAK2, JCP405 and JPM-OEt and then labeled with FY01. Schizonts were lysed, and soluble (top gels) and insoluble (middle gels) pellet fractions were analyzed separately. Nonidet P-40-insoluble extracts from purified merozoites were similarly analyzed (bottom gels). The location of labeled DPAP1, DPAP3 and falcipains are shown. **(d)** Schizonts (36 h post invasion) were treated with SAK1 and SAK2 (1–100 μ M) for 24 h and stained with propidium iodide, and schizonts were quantified relative to the DMSO control. Standard error for triplicate runs are shown. **(e)** Giemsa-stained thin blood smears of cultures treated with 10 μ M of the DPAP-selective inhibitors SAK1 and SAK2 and the general papain-family inhibitor JPM-OEt.

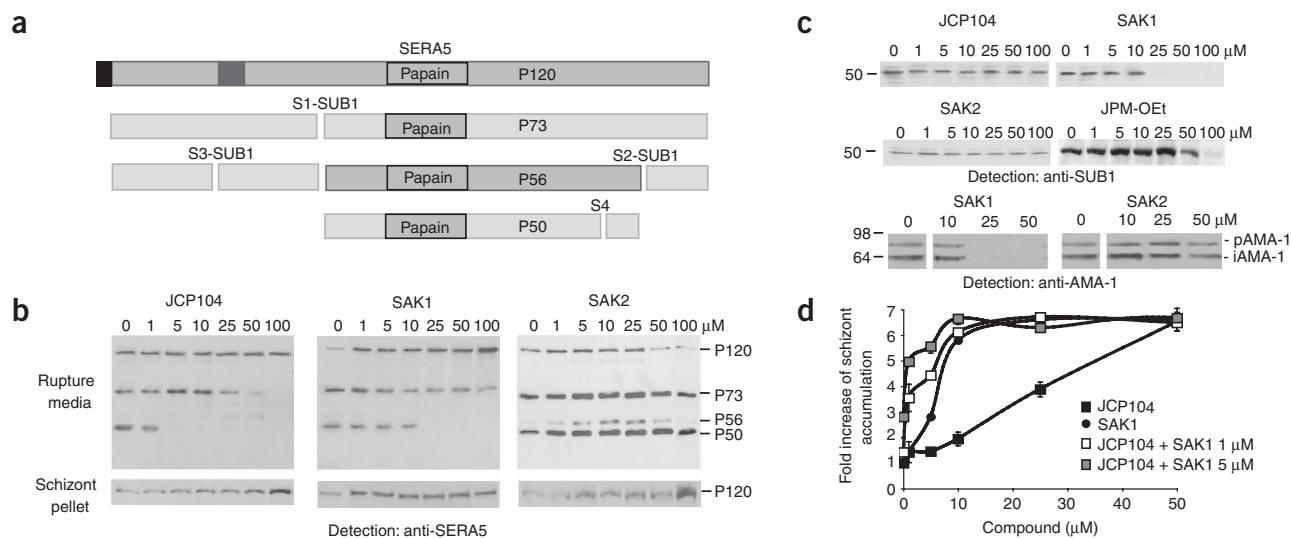


Figure 6 PfSUB1 and DPAP3 mediate SERA5 processing. **(a)** Schematic of SERA5 processing sites including the S1–S4 cleavage sites. The papain-family protease domain is shown, along with the signal peptide (black) and transmembrane domain (dark gray). **(b)** Effects of PfSUB1 and DPAP inhibitors on SERA5 processing. Schizonts (36–40 h post invasion) were treated for 6–8 h with JCP104, SAK1 and SAK2 (at indicated concentrations). The schizont pellet and medium were collected and separated by 8% SDS-PAGE. SERA5 was detected by western blot. **(c)** Samples in **b** were analyzed by blot using a PfSUB1-specific rabbit antibody. Samples from cells treated as in **a** with a range of concentrations of JPM-OEt are also shown. Similar samples from parasites treated with SAK1 and SAK2 at the indicated concentrations were analyzed by blot using an AMA-1-specific rabbit antibody. The precursor form (pAMA-1) and an intermediate form (iAMA-1) before final processing to the mature secreted form are indicated. **(d)** Synergistic effects of SAK1 and JCP104 on schizont rupture. Schizonts (36 h post invasion) were treated with a set concentration of SAK1 (1 μM) and then treated with a range of concentrations of JCP104 (1–100 μM). Average values for fold increase in schizont accumulation relative to controls are plotted. Experiments were performed in triplicate, and standard error bars are shown.

DPAP1 and DPAP3, and also to determine the extent of cross-reactivity of the compounds toward the falcipains (Fig. 5c). The DPAP1-selective inhibitor SAK2 was a highly potent inhibitor of DPAP1 and falcipain-1 and showed only weak inhibition of falcipain-2 and falcipain-3. SAK2 showed activity against DPAP3 only at the highest concentrations tested. SAK1, on the other hand, was a highly potent inhibitor of DPAP3 and showed only very weak activity toward DPAP1. SAK1 was also a weak inhibitor of all of the falcipains relative to the E-64 analog JPM-OEt (19)³¹, which blocked labeling of all three falcipains even at the lowest concentration of compound tested.

Having confirmed the specificity of SAK1 and SAK2, we carried out a dose-response study of the compounds in the rupture assay (Fig. 5d). The DPAP3-selective compound SAK1 produced a potent dose-dependant accumulation of schizonts at concentrations nearly identical to those observed for the original nonspecific hits JCP405 and JCP410. However, the DPAP1-selective compound SAK2 showed weak effects, with minimal accumulation of schizonts below the high concentrations at which it shows cross-reactivity with DPAP3. Since the original hit JCP405 blocks DPAP1 labeling to the same extent as SAK2, the difference in potency of these two compounds in the rupture assay can only be explained by their large difference in potency toward DPAP3 (Fig. 5c). In addition, the fact that JCP405 and SAK1 have similar overall potency in the rupture assay but have markedly different potency toward the falcipains suggests that the combined inhibition of DPAP3 and the falcipains is not required for efficient effects on rupture. Finally, to further rule out the possibility that the rupture effects of SAK1 were mediated by its cross-reactivity with falcipain-2 and falcipain-3, we examined the effects of SAK1, SAK2 and JPM-OEt by Giemsa stained thin blood film analyses of schizonts treated at 36 h post invasion at a concentra-

tion of 10 μM (Fig. 5e). Staining of the treated parasites revealed that SAK1 caused substantial accumulation of mature schizonts, whereas SAK2 had virtually no effect and JPM-OEt caused an accumulation of parasites with a swollen food vacuole. Thus, these combined data suggest that DPAP3 is the target mediating the rupture effects of our hits.

Inhibition of PfSUB1 or DPAP3 blocks SERA5 processing

Having identified two protease targets that regulate the rupture process, we turned our attention to defining the mechanism of this regulation. We initially chose to focus on the SERAs, since these highly abundant proteins are found in the parasitophorous vacuole and are proteolytically processed and released during rupture^{11,33,34}. Several studies have also linked these proteins to the process of host cell rupture^{9,13}. Of this family of nine proteins, only SERA3, SERA4, SERA5, SERA6 and SERA9 are detectably expressed at the protein level in the blood stages¹⁰. Of these, SERA5 is the most abundantly expressed family member and seems to be essential for normal blood-stage growth^{10,12}. Furthermore, data have confirmed that recombinant PfSUB1 is capable of processing SERA5 at the same sites observed *in vivo*²³. Therefore, we decided to focus our efforts on the analysis of SERA5.

SERA5 is expressed as a 120 kDa precursor protein (P120) that is proteolytically processed to a P73 form, a P56 form and ultimately a P50 form that is released during host cell rupture (Fig. 6a)¹¹. Initial processing occurs at the S1 site to generate the P73 intermediate and then at the S2 site to generate the P56 form. Processing at both the S1 and S2 sites can be blocked by serine protease inhibitors¹¹. Further processing of the P56 form to the P50 form is sensitive to cysteine protease inhibitors¹¹. We therefore examined whether inhibition of PfSUB1 or DPAP3 in late-stage schizonts has an effect on processing

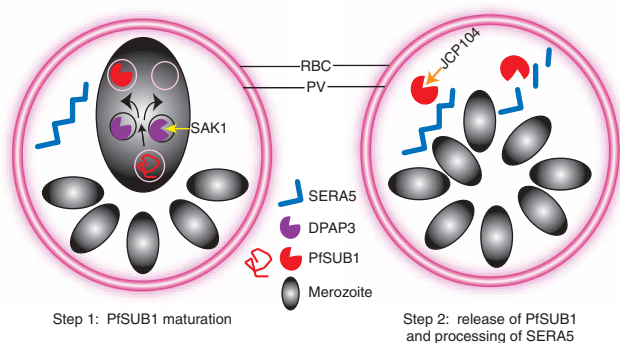


Figure 7 The protease pathway involved in schizont rupture. Possible mechanism used by DPAP3 and PfsUB1 to regulate host cell rupture. Step 1: maturation of PfsUB1, which can be blocked by the DPAP3-selective inhibitor SAK1. Step 2: release of PfsUB1 into the parasitophorous vacuole (PV) and subsequent proteolysis of SERA5, which can be directly blocked by the inhibitor JCP104.

of this protein. We monitored the composition of SERA5 species both in the pellet and in the rupture media from cultures treated with a range of concentrations of JCP104, SAK1 and SAK2 (**Fig. 6b**). Both JCP104 and SAK1 caused a dose-dependent accumulation of the precursor P120 and P73 forms and complete loss of production of the P50 form. Notably, SAK2 caused accumulation of precursor P120 only when used at the highest concentration for which it showed cross-reactivity with DPAP3. Given that SERA5 processing was blocked at the P73 stage when low (subsaturating) concentrations of JCP104 were used (**Fig. 6b**), we hypothesized that partial block or partial reduction in levels of PfsUB1 could result in incomplete processing of SERA5. Therefore, we decided to investigate whether inhibition of DPAP3 was affecting SERA5 processing by reducing the levels of active PfsUB1. We analyzed levels of mature PfsUB1 in the same pellet fractions used for the SERA5 analysis (**Fig. 6c**). The DPAP3-selective inhibitor SAK1 substantially blocked the production of P54 at the same concentrations of the drug required to reduce SERA5 processing and to induce robust effects on host cell rupture. We were unable to detect any accumulation of the P80 precursor of PfsUB1, which suggests that DPAP3 may regulate the folding and activation of PfsUB1 and that intermediates of PfsUB1 may be rapidly degraded. Importantly, the DPAP1-selective inhibitor SAK2 failed to reduce levels of mature PfsUB1, and the highly potent falcipain inhibitor JPM-OEt only reduced levels at concentrations at which it also blocks DPAP3 activity (**Fig. 6c**). To further investigate the potential role of DPAP3 as a general maturase of proteins destined for secretory vesicles, we analyzed the levels of the well-characterized microneme protein AMA-1. This protein is proteolytically processed multiple times during trafficking to and secretion from the micronemes during rupture and invasion⁸. Treatment of parasites with the DPAP3-specific inhibitor SAK1 caused a complete loss of detection of the precursor and intermediate forms of AMA-1, whereas the DPAP1-selective compound had virtually no effect on the levels of these proteins (**Fig. 6c**). As observed for PfsUB1, inhibition of DPAP3 did not result in the accumulation of immature precursor form of the AMA-1, which suggests that DPAP3 function may be generally required for proper folding and stabilization of this secretory protein.

Finally, to confirm that DPAP3 functions upstream of PfsUB1, we tested the ability of SAK1 to enhance the potency of JCP104 in the

rupture assays. We reasoned that intermediate concentrations of SAK1 should induce a reduction in the amount of mature PfsUB1, thereby leading to enhanced potency of JCP104 in the assay. When cells were treated with fixed concentrations of SAK1 and then treated with a range of concentrations of JCP104 (1–100 μM), the dose-response curves showed a substantial shift to the lower concentration ranges, which suggests that the compounds may behave in a synergistic way when used in combination (**Fig. 6d**). We also used the data from the combination treatment studies to generate an isobologram³⁵ (**Supplementary Fig. 7** online) to confirm that the compounds act synergistically, as would be expected for inhibitors that target multiple proteases in a related biological pathway.

DISCUSSION

Proteases have important regulatory roles in many diverse cellular processes. Not surprisingly, the parasite *P. falciparum* uses proteases at various points during both the blood stage and insect stage of its life cycle. In this study, we screened a highly focused library of covalent serine and cysteine protease inhibitors in a cell-based assay that allowed us to monitor changes in life cycle progression. From this screen, we identified serine and cysteine protease inhibitors that had specific, dose-dependent effects on host cell rupture. Due to the covalent nature of the inhibition mechanism of these compounds, we were able to identify the serine protease PfsUB1 and the cysteine protease DPAP3 as the targets of these compounds. Furthermore, we were able to correlate potency of inhibition of each protease target with potency in the rupture assay, thus confirming their functional roles in this process. In addition, the inhibitors used in the target identification phase could also be applied to studies of the mechanism of the rupture process.

Based on our combined data, we have developed a model that proposes how two mechanistically distinct proteases, PfsUB1 and DPAP3, regulate the process of rupture of merozoites from host red blood cells (**Fig. 7**). In this model, PfsUB1 is synthesized as a precursor protein in vesicles within the secretory pathway. These immature forms of PfsUB1 are then trafficked to or through vesicles containing DPAP3, where the precursor then matures to the active P47 form. Finally, just before rupture, mature PfsUB1 is released into the parasitophorous vacuole, where it directly mediates processing of SERA5.

As we analyzed our initial screening data and began to come to the conclusion that PfsUB1 is the most likely target of JCP104, another laboratory was nearing completion of its own study that suggested that PfsUB1 is a regulator of host cell rupture and that it mediates its effects by processing of the parasitophorous vacuole protein SERA5 (ref. 23). These studies confirmed that recombinant PfsUB1 directly processes SERA5 at both the S1 and S2 sites. Furthermore, analysis of the cleavage site sequences of SERA5 identified a consensus sequence for optimal PfsUB1 binding that contains a P4 hydrophobic residue, a P2 small amino acid and a P1 polar residue. Importantly, PfsUB1 processing of the S2 site is substantially slower than processing at the S1 site, perhaps explaining why inhibitors of DPAP3 that reduce, but do not completely block, production of PfsUB1 cause accumulation of the P73 intermediate of SERA5.

The production of mature PfsUB1 involves the initial synthesis of a P80 precursor that is rapidly processed to a P54 intermediate and is finally processed to the mature P47 form²⁰. Since inhibition of DPAP3 leads to complete loss of formation of the intermediate P54 form of PfsUB1 without the accumulation of precursors, we believe that the DPAP3 may be required for its maturation, and failure to process these intermediates may lead to their rapid degradation. Although the

first step of PfSUB1 maturation is known to be an autocatalytic, intramolecular cleavage event³⁶, the second P54-to-P47 step of PfSUB1 maturation is less well understood and could be regulated either directly or indirectly by DPAP3. Our data for AMA-1 (Fig. 6c) suggest that DPAP3 may be a general maturase enzyme that controls processing and activation of secretory proteins through processing or activation of other targets that mediate trafficking or folding of secretory proteins. It is notable that mammalian cathepsin C (a close homolog of the DPAPs) is located in the secretory granules of mast cells, where it regulates the levels of secretory proteases³⁷. In further support of this, analysis of green fluorescent protein (GFP)-DPAP3-expressing parasites suggests that DPAP3 has a punctate, vesicular staining pattern in merozoites (M. Klemba, Virginia Tech, personal communication). This also fits with the recent identification of exonemes and the demonstration that these specialized secretory vesicles contain PfSUB1 (ref. 23).

Although it is clear that PfSUB1 maturation and activity are essential for parasite rupture, the question remains whether PfSUB1 cleavage of SERA5 leads to its activation as a protease that plays an active role in the rupture process. Considering that the SERAs all have a conserved papain protease fold domain, it is tempting to propose that processing of the precursor forms of SERA5 leads to its activation as a protease. Evidence for weak chymotrypsin activity has been demonstrated for the P50 form of SERA5 (ref. 38), perhaps due to the use of suboptimal peptide substrates. It is also possible that SERA5 has hydrolase activity against non-protein substrates. In fact, lipases and several other classes of hydrolytic enzymes contain folds that are similar to proteases. Clearly additional studies will be required to determine whether the 'catalytic' residues of SERA5 are required for its function, although this will most likely require difficult and time-consuming genetic knock-in experiments.

The DPAP proteases are a potentially useful class of enzymes for drug development efforts. Our work here shows that the DPAP3 family member is expressed in an active form and that in merozoites, multiple processed forms of DPAP3 exist. Because the related DPAP1 protease has an essential role in end-stage hemoglobin degradation²⁹, compounds that block both of these proteases are likely to have significant effects on parasite metabolism and on host cell rupture. In addition, our results using a combination of DPAP3 and PfSUB1 inhibitors suggest that a multitarget approach may be optimal in order to reduce the chances of parasite resistance to this treatment strategy.

The results presented here identify specific proteases involved in the regulation of host cell rupture by the malaria parasite and explain the inhibition effects obtained with broad-spectrum inhibitors. Because parasites must efficiently rupture host cells not only during the blood-stage infection but also after initial invasion of cells of the liver and during the oocyst stage in the insect, we believe that inhibitors of proteases that have important roles in the general rupture process have the potential to be effective at each of these stages of the parasite infective cycles. Work is currently underway to test DPAP3 and PfSUB1 inhibitors in mouse models of malaria and in insect stages to determine whether this process of regulation of host cell rupture is a general phenomenon.

METHODS

Parasite culture, harvesting life stages and preparation of lysates. For details see **Supplementary Methods** online.

Assembly of the directed protease inhibitor library. Directed irreversible inhibitors of serine and cysteine proteases were acquired as generous gifts from J. Powers and W. Roush. The 1,211 compounds were manually dissolved to

50 mM concentrations in DMSO and subsequently diluted to 10 mM and 1 mM concentrations in 96-well plates. The database of compounds and their respective results from the high-throughput screening were compiled in the Collaborative Drug Discovery, Inc. database.

Phenotypic screen for rupture defect using flow cytometry. Synchronous early schizonts (~36 h post invasion) were treated with the library of directed irreversible inhibitors at a final concentration of 10 μ M for 24 h at 37 °C in a 96-well-plate format and then fixed with 0.05% glutaraldehyde (Sigma) in 1 \times phosphate-buffered saline (PBS) overnight at 4 °C. The fixed cells were permeabilized with 0.25% Triton X-100 for 5 min at room temperature (25 °C) and stained with a 1:100 dilution of a 5 mg ml⁻¹ working solution of propidium iodide (Sigma) in deionized water. Progression of the parasite life cycle was monitored by observation of distinct propidium iodide-stained populations using a BD FACScan flow cytometer (Becton, Dickinson and Co.) located in the Stanford Shared FACS Facility at Stanford University. The data obtained were analyzed for the ring-stage and schizont-stage populations using FlowJo 6.4.2. In general, ring stages were defined as 200–800 on the forward scatter and 200–800 on the fluorescence axis, whereas schizont stages were defined as 100–600 on the forward scatter and 1,000–6,000 on the fluorescence axis. The location of the ring stages was always confirmed with the dot plot of the DMSO controls on the respective plates. There were an average of 10 DMSO controls per compound plate. The data from each of the DMSO controls was averaged, and any data points more than 2 s.d. for the average were discarded. The populations were converted to fractions of the total parasitemia per well. These values were then normalized to the respective averaged populations of the DMSO control. Samples with an accumulation had a value greater than 1, samples with a depletion had a value less than 1 and samples similar to the control had a value approximately equal to 1. Screening was performed in triplicate, and compounds exhibiting a schizont accumulation greater than or equal to 1.4-fold above the DMSO control in at least two runs were considered as preliminary hits.

Triaging of the preliminary hits. Preliminary hits were evaluated for reproducibility, blood smear phenotype, compound purity and stability, life cycle stage specificity and toxicity. Preliminary hit compounds were tested for reproducibility by flow cytometry, as described above, and the results were corroborated by Giemsa-stained thin blood smears. Reproducible hit compounds from the library were tested for initial purity and then stability in aqueous solution (200 mM phosphate buffer, pH 7.0) for 8 and 24 h at 37 °C using LC/MS (liquid chromatography, Agilent 1100 Series, and mass spectrometry, API 150EX, Applied Biosystems). The remaining compounds were used to treat synchronous ring-stage parasites (10 μ M final concentration) and analyzed 24 h later by Giemsa-stained thin blood smear to further eliminate compounds that had additional nonspecific effects on parasite development. General toxicity was further analyzed by repeating the initial schizont screening conditions, described above, but increasing the treatment to 50 μ M final concentration of the compounds. Parasites were analyzed by Giemsa-stained thin blood smears to determine general toxicity to the host red blood cells, exhibited by hemolysis, or general toxicity to the parasites, exhibited by death of the parasite population. All compounds were simultaneously screened for general toxicity by the CellTiter-Glo luminescent cell viability assay (Promega) using BSC-1 cells (epithelial cells of African green monkey kidney origin). The data were collected on a SpectraMax M5 (Molecular Devices).

Labeling and competition for labeling of proteases with activity-based probes. Protease activities were visualized using fluorophore, biotin or ¹²⁵I-radiolabeled tags on activity-based probes (ABPs) that covalently modify the active site of the target proteases. All inhibitor competitions for ABP labeling were performed by 30 min of inhibitor treatment at room temperature followed by 1 h probe labeling at room temperature. The reactions were subsequently quenched with an SDS loading buffer and boiling before separation by SDS-PAGE. For probing asynchronous parasite, schizont, or merozoite lysates, 50 μ g of total protein as determined by Bradford Coomassie protein assay reagent (Pierce) was diluted to 50 μ l in reaction buffer consisting of the same composition as the pH 7.4 or 5.5 lysis buffers described above minus the 1% nonidet P-40. Intact schizont labeling

was performed using 1×10^8 percoll-enriched schizonts resuspended in serum-free RPMI (Invitrogen) at a final volume of 50 μ l. SLO-lysed schizonts were labeled using 1×10^8 percoll-enriched schizonts treated with SLO resuspended in reaction buffer at a final volume of 50 μ l. ABPs with a biotin tag were detected by standard western blotting procedures using a streptavidin-HRP antibody (Sigma). Probes with an 125 I label were detected by exposing dried SDS-PAGE gels to an autoradiography screen overnight at room temperature, whereas probes with a BODIPY-TMR fluorescent tag were directly imaged in SDS-PAGE gels. Both the iodinated and fluorescent probes were imaged on a 9410 Typhoon Scanner (Amersham Biosciences, GE Healthcare).

Streptavidin affinity purification and PfSUB1 detections. Frozen saponin-lysed schizont pellets were lysed in pH 7.4 lysis buffer for 1 h on ice (at 0 °C) and centrifuged at 10,000 r.p.m. in a microcentrifuge, and the soluble fraction was collected. 300 μ g of lysate was then precleared with streptavidin beads (Pierce) for 1 h at room temperature and probed with 1 μ M JCP104. The labeled proteins were pulled down overnight at 4 °C with streptavidin beads and eluted by boiling in SDS loading buffer. The eluted proteins were separated on a 12% SDS-PAGE gel. Western blot analyses for PfSUB-1 were done using a polyclonal anti-SUB1 antibody raised in mouse or rabbit²². A rabbit polyclonal anti-SUB2 antibody was used as a negative control³⁹.

Construction of the FY01 library, screening in gel-based assays, and synthesis of SAK1 and SAK2. A directed library of 40 compounds based on the FY01 scaffold with the P1 residue fixed as homophenylalanine and varying P2 with 20 natural and 20 non-natural compounds was generated using solid-phase synthesis described previously³². The library was used at 100 μ M for competition studies with the FY01 probe in asynchronous culture and merozoite lysates prepared at pH 5.5. The residual activities of the DPAPs treated with the inhibitors were assessed by Image J 1.37 software (<http://rsb.info.nih.gov/ij/download.html>), and the data of two runs was visualized with a heat map using Cluster and Java TreeView 1.0.8 (<http://bonsai.ims.u-tokyo.ac.jp/~mdehoon/software/cluster/>). Selectivity of the compounds toward the falcipains was also assessed using the general papain-family cysteine protease probe 125 I-DCG04 (ref. 31). SAK1 and SAK2 were synthesized in solution-phase using standard chemistries described for the synthesis of vinyl sulfones⁴⁰.

SERA processing assay. Percoll-enriched schizonts were incubated in serum-free RPMI medium for 6–8 h. The collected medium was fractionated on an 8% SDS-PAGE gel, and SERA5 was detected by western blotting using the SERA5-specific monoclonal antibody 24C6.1F1 (ref. 41), a gift from J.-F. Dubremetz, which recognizes an epitope within the P50 processing product. The schizont pellet was directly solubilized in 10 \times volume of 2 \times SDS-PAGE loading buffer and analyzed by western blotting for SERA5 and PfSUB1 anti-sera.

Note: Supplementary information and chemical compound information is available on the Nature Chemical Biology website.

ACKNOWLEDGMENTS

The authors thank M. Blackman (UK National Institute for Medical Research) for sharing his data on SERA5 processing before its publication and for providing reagents for PfSUB1. We also thank M. Klemba (Virginia Tech) for valuable information about the DPAPs and the DPAP1-specific antibodies. We thank J. Powers (University of Georgia) and W. Roush (The Scripps Research Institute) for the directed irreversible inhibitors of serine and cysteine proteases. We thank J.-F. Dubremetz (Université de Montpellier 2) for providing the SERA5-specific antibody. We thank C. Yang for generating compound toxicity data, S. Verhelst for analysis of NMR data and A. Guzzetta for high-resolution mass spectrometry analysis of compounds. This work was supported by funding from the Kinship Foundation as part of the Searle Scholars program (to M.B.), from a Burroughs Wellcome Trust New Investigators in Pathogenesis Award (to M.B.) and by the US National Institutes of Health National Technology Center for Networks and Pathways grants U54 RR020843 and R01 EB005011 (to M.B.). S.A.K. is supported by the US National Institutes of Health Research Fellowship Award F32 AI069728-01A1. E.L.P. is supported by the US National Science Foundation Graduate Research Fellowship 2005021299. C.I.P. is supported by an American Society for Microbiology Watkins Fellowship.

Published online at <http://www.nature.com/naturechemicalbiology>
Reprints and permissions information is available online at <http://npg.nature.com/reprintsandpermissions>

- Carruthers, V.B. & Blackman, M.J. A new release on life: emerging concepts in proteolysis and parasite invasion. *Mol. Microbiol.* **55**, 1617–1630 (2005).
- O'Donnell, R.A. & Blackman, M.J. The role of malaria merozoite proteases in red blood cell invasion. *Curr. Opin. Microbiol.* **8**, 422–427 (2005).
- Rosenthal, P.J. Cysteine proteases of malaria parasites. *Int. J. Parasitol.* **34**, 1489–1499 (2004).
- Wickham, M.E., Culvenor, J.G. & Cowman, A.F. Selective inhibition of a two-step egress of malaria parasites from the host erythrocyte. *J. Biol. Chem.* **278**, 37658–37663 (2003).
- Harris, P.K. *et al.* Molecular identification of a malaria merozoite surface sheddase. *PLoS Pathog.* **1**, 241–251 (2005).
- Green, J.L., Hinds, L., Grainger, M., Knuepfer, E. & Holder, A.A. Plasmodium thrombospondin related apical merozoite protein (PTRAMP) is shed from the surface of merozoites by PfSUB2 upon invasion of erythrocytes. *Mol. Biochem. Parasitol.* **150**, 114–117 (2006).
- Li, J., Mitamura, T., Fox, B.A., Bzik, D.J. & Horii, T. Differential localization of processed fragments of *Plasmodium falciparum* serine repeat antigen and further processing of its N-terminal 47 kDa fragment. *Parasitol. Int.* **51**, 343–352 (2002).
- Howell, S.A. *et al.* Distinct mechanisms govern proteolytic shedding of a key invasion protein in apicomplexan pathogens. *Mol. Microbiol.* **57**, 1342–1356 (2005).
- Aly, A.S. & Matuschewski, K. A malarial cysteine protease is necessary for *Plasmodium* sporozoite egress from oocysts. *J. Exp. Med.* **202**, 225–230 (2005).
- Miller, S.K. *et al.* A subset of *Plasmodium falciparum* SERA genes are expressed and appear to play an important role in the erythrocytic cycle. *J. Biol. Chem.* **277**, 47524–47532 (2002).
- Li, J., Matsuoka, H., Mitamura, T. & Horii, T. Characterization of proteases involved in the processing of *Plasmodium falciparum* serine repeat antigen (SERA). *Mol. Biochem. Parasitol.* **120**, 177–186 (2002).
- Aoki, S. *et al.* Serine repeat antigen (SERA5) is predominantly expressed among the SERA multigene family of *Plasmodium falciparum*, and the acquired antibody titers correlate with serum inhibition of the parasite growth. *J. Biol. Chem.* **277**, 47533–47540 (2002).
- Pang, X.L., Mitamura, T. & Horii, T. Antibodies reactive with the N-terminal domain of *Plasmodium falciparum* serine repeat antigen inhibit cell proliferation by agglutinating merozoites and schizonts. *Infect. Immun.* **67**, 1821–1827 (1999).
- Blackman, M.J. Purification of *Plasmodium falciparum* merozoites for analysis of the processing of merozoite surface protein-1. *Methods Cell Biol.* **45**, 213–220 (1994).
- Contreras, C.E. *et al.* Stage-specific activity of potential antimalarial compounds measured *in vitro* by flow cytometry in comparison to optical microscopy and hypoxanthine uptake. *Mem. Inst. Oswaldo Cruz* **99**, 179–184 (2004).
- Powers, J.C., Asgian, J.L., Ekici, O.D. & James, K.E. Irreversible inhibitors of serine, cysteine, and threonine proteases. *Chem. Rev.* **102**, 4639–4750 (2002).
- Jackson, K.E. *et al.* Selective permeabilization of the host cell membrane of *Plasmodium falciparum*-infected red blood cells with streptolysin O and equinatoxin II. *Biochem. J.* **403**, 167–175 (2007).
- Saliba, K.J. & Kirk, K. Nutrient acquisition by intracellular apicomplexan parasites: staying in for dinner. *Int. J. Parasitol.* **31**, 1321–1330 (2001).
- Nyalwidhe, J. *et al.* A nonpermeant biotin derivative gains access to the parasitophorous vacuole in *Plasmodium falciparum*-infected erythrocytes permeabilized with streptolysin O. *J. Biol. Chem.* **277**, 40005–40011 (2002).
- Sajid, M., Withers-Martinez, C. & Blackman, M.J. Maturation and specificity of *Plasmodium falciparum* subtilisin-like protease-1, a malaria merozoite subtilisin-like serine protease. *J. Biol. Chem.* **275**, 631–641 (2000).
- Jean, L., Withers-Martinez, C., Hackett, F. & Blackman, M.J. Unique insertions within *Plasmodium falciparum* subtilisin-like protease-1 are crucial for enzyme maturation and activity. *Mol. Biochem. Parasitol.* **144**, 187–197 (2005).
- Blackman, M.J. *et al.* A subtilisin-like protein in secretory organelles of *Plasmodium falciparum* merozoites. *J. Biol. Chem.* **273**, 23398–23409 (1998).
- Yeoh, S. *et al.* Subcellular discharge of a serine protease mediates release of invasive malaria parasites from host erythrocytes. *Cell* **131**, 1072–1083 (2007).
- Shenai, B.R., Sijwali, P.S., Singh, A. & Rosenthal, P.J. Characterization of native and recombinant falcipain-2, a principal trophozoite cysteine protease and essential hemoglobinase of *Plasmodium falciparum*. *J. Biol. Chem.* **275**, 29000–29010 (2000).
- Sijwali, P.S., Shenai, B.R., Gut, J., Singh, A. & Rosenthal, P.J. Expression and characterization of the *Plasmodium falciparum* haemoglobinase falcipain-3. *Biochem. J.* **360**, 481–489 (2001).
- Sijwali, P.S. & Rosenthal, P.J. Gene disruption confirms a critical role for the cysteine protease falcipain-2 in hemoglobin hydrolysis by *Plasmodium falciparum*. *Proc. Natl. Acad. Sci. USA* **101**, 4384–4389 (2004).
- Sijwali, P.S., Koo, J., Singh, N. & Rosenthal, P.J. Gene disruptions demonstrate independent roles for the four falcipain cysteine proteases of *Plasmodium falciparum*. *Mol. Biochem. Parasitol.* **150**, 96–106 (2006).
- Kam, C.M. *et al.* Design and evaluation of inhibitors for dipeptidyl peptidase I (Cathepsin C). *Arch. Biochem. Biophys.* **427**, 123–134 (2004).

29. Klemba, M., Gluzman, I. & Goldberg, D.E. A *Plasmodium falciparum* dipeptidyl aminopeptidase I participates in vacuolar hemoglobin degradation. *J. Biol. Chem.* **279**, 43000–43007 (2004).
30. Yuan, F., Verhelst, S.H., Blum, G., Coussens, L.M. & Bogyo, M. A selective activity-based probe for the papain family cysteine protease dipeptidyl peptidase I/cathepsin C. *J. Am. Chem. Soc.* **128**, 5616–5617 (2006).
31. Greenbaum, D.C. *et al.* A role for the protease falcipain 1 in host cell invasion by the human malaria parasite. *Science* **298**, 2002–2006 (2002).
32. Wang, G., Mahesh, U., Chen, G.Y. & Yao, S.Q. Solid-phase synthesis of peptide vinyl sulfones as potential inhibitors and activity-based probes of cysteine proteases. *Org. Lett.* **5**, 737–740 (2003).
33. Delplace, P., Fortier, B., Tronchin, G., Dubremetz, J.F. & Vernes, A. Localization, biosynthesis, processing and isolation of a major 126 kDa antigen of the parasitophorous vacuole of *Plasmodium falciparum*. *Mol. Biochem. Parasitol.* **23**, 193–201 (1987).
34. Delplace, P. *et al.* Protein p126: a parasitophorous vacuole antigen associated with the release of *Plasmodium falciparum* merozoites. *Biol. Cell* **64**, 215–221 (1988).
35. Tallarida, R.J. Drug synergism: its detection and applications. *J. Pharmacol. Exp. Ther.* **298**, 865–872 (2001).
36. Withers-Martinez, C. *et al.* Expression of recombinant *Plasmodium falciparum* subtilisin-like protease-1 in insect cells. Characterization, comparison with the parasite protease, and homology modeling. *J. Biol. Chem.* **277**, 29698–29709 (2002).
37. Henningsson, F., Wolters, P., Chapman, H.A., Caughey, G.H. & Pejler, G. Mast cell cathepsins C and S control levels of carboxypeptidase A and the chymase, mouse mast cell protease 5. *Biol. Chem.* **384**, 1527–1531 (2003).
38. Hodder, A.N. *et al.* Enzymic, phylogenetic, and structural characterization of the unusual papain-like protease domain of *Plasmodium falciparum* SERA5. *J. Biol. Chem.* **278**, 48169–48177 (2003).
39. Hackett, F., Sajid, M., Withers-Martinez, C., Grainger, M. & Blackman, M.J. PfSUB-2: a second subtilisin-like protein in *Plasmodium falciparum* merozoites. *Mol. Biochem. Parasitol.* **103**, 183–195 (1999).
40. Palmer, J.T., Rasnick, D., Klaus, J.L. & Bromme, D. Vinyl sulfones as mechanism-based cysteine protease inhibitors. *J. Med. Chem.* **38**, 3193–3196 (1995).
41. Delplace, P., Dubremetz, J.F., Fortier, B. & Vernes, A. A 50 kilodalton exoantigen specific to the merozoite release-reinvasion stage of *Plasmodium falciparum*. *Mol. Biochem. Parasitol.* **17**, 239–251 (1985).